COBEM 2023 27TH INTERNATIONAL CONGRESS OF MECHANICAL ENGENEERING

ABCM Brazilian Society of Mechanical Sciences and Engineering
27th ABCM International Congress of Mechanical Engineering
December 04-08, 2023, Florianópolis-SC, Brazil

COB-2023-0581
Experimental investigation into the impact of stage number on the performance of ESP operating with a gas-liquid mixture.

Yan Caires Capellaro
yanccapellaro@outlook.com
School of Mechanical Engineering, University of Campinas - Cidade Universitária Zeferino Vaz - Barão Geraldo, Campinas - SP, 13083-970
William Monte Verde
wmv@unicamp.com
Center for Petroleum and Energy Studies - Rua Cora Coralina, 350, Cidade Universitária, Campinas, São Paulo, Brazil, 13083-896
Rafael Franklin Lazaro de Cerqueira
rafael.cerqueira@ufsc.br
SINMEC - Computational Fluid Dynamics Lab, Mechanical Engineering Department, Federal University of Santa Catarina, Florianopolis - SC, 88040-900, Brazil
Julio Picinato Orssatto
jporssatto@gmail.com
School of Mechanical Engineering, University of Campinas - Cidade Universitária Zeferino Vaz - Barão Geraldo, Campinas - SP, 13083-970
Bernardo Pereira Foresti
foresti@petrobras.com.br
Petrobras/CENPES - Av. Horácio Macedo, 950 - Cidade Universitária da Universidade Federal do Rio de Janeiro, Rio de Janeiro - RJ, 21941-915
Antonio Carlos Bannwart
bannwart@unicamp.br
Center for Petroleum and Energy Studies - Rua Cora Coralina, 350, Cidade Universitária, Campinas, São Paulo, Brazil, 13083-896
Marcelo Souza de Castro
mscastro@unicamp.br
School of Mechanical Engineering, University of Campinas - Cidade Universitária Zeferino Vaz - Barão Geraldo, Campinas - SP, 13083-970

Abstract. *ESPs are one of the most widely used equipments for artificial lifting. However, their performance is greatly affected by the presence of gas in the working fluid. In oil production, the operating conditions are fundamental for an economically viable well, so understanding phenomena such as surging and gas locking is an important piece of the puzzle in solving the problems when a compressible phase is present in the working fluid. Several studies present the operating parameters, such as rotor geometry, viscosity, etc., in an isolated manner. In this study, the authors aim to investigate the effects of different numbers of stages on ESP performance degradation and the ability of a convolutional neural network to predict flow patterns based on images of the inside of an impeller. A prototype based on a modified ESP P23 has been built in order to vary the number of stages in a modular way, being able to accommodate four different configurations, with 1, 2, 3 and 4 stages. The modified pump also has two visualization windows, allowing to visualize the inside of one of the stages, which is the last in the assembled system, and the inlet of the first stage. Using two high-speed cameras, one for each visualization section, and measuring the pump pressure stage by stage, the tests were carried out with a wide range of gas flow rates, liquid flow rates, four different stage configurations and three different ESP shaft speeds. Results show that the deterioration in the performance of the pump under gas-liquid flow increases as its number of stages decreases. This is particularly the case at lower speeds, with flow pattern transitions being dislocated, occurring with lower gas flow rates, the presence of larger bubbles are also observed the lower the stage count. Surging and gas blocking effects also occur earlier and more severely with fewer stages.*

Keywords: *Electric Submersible Pump, Two-phase Flow, Gas-Liquid Flow, Flow Visualization*

1. INTRODUCTION

The Electrical Submersible Pump (ESP) is an important artificial lift method used in the oil industry. Zhu *et al.* (2019) ranked the ESP as the second most used method, being the first in terms of volume of production. The ESP method is known for its flexibility and high production potential. However, ESP suffers from a major drawback due to the high workover cost, especially in offshore applications with wet Christmas trees. Hence, proper ESP system design

and production monitoring are essential to increase its lifetime and reliability. Therefore, understanding how operational variables influence ESP operation is imperative.

The number of pump stages is an important variable in the design of an ESP, particularly in the context of two-phase gas-liquid flow. This parameter can significantly impact ESP performance, and being an understudied topic in the literature further in-depth analysis is required. Preliminary findings and conclusions from specific studies suggest that a higher number of stages enhances an ESP's ability to handle free gas (Cirilo, 1998).

The ESP operating with a gas-liquid mixture is susceptible to two main phenomena, as described by Gamboa (2009): Surging and Gas Locking. Surging is usually associated with the flow pattern transition between Dispersed Bubbles to Agglomerated Bubbles, as observed by Zapata (2003) and Monte Verde (2016). When surging occurs, the pump's performance is severely affected, and its capacity to generate head is reduced. Zapata (2003) describes gas locking as the occurrence of larger gas bubbles inside the pump's impellers, leading to a complete degradation in its performance, resulting in a null head, and consequently in a null flow rate.

The ESP performance operating with two-phase gas-liquid flow is described by Gamboa and Prado (2011) based on two tests: surging and mapping. In the surging test, liquid flow rate is held constant while the gas flow rate is increased. On the other hand, the mapping test maintains a constant gas flow rate while varying the liquid flow rate within an expected range, typically from the open-flow point (zero pressure gain) to the shutoff point (zero flow rate). Both of these tests are extensively utilized in the study of ESPs.

Monte Verde (2016) provided a comprehensive description and classification of the flow patterns observed within a visualization impeller. The categorization, similar to the findings of Gamboa (2009), identifies four distinct gas-liquid flow patterns: Dispersed Bubbles, Agglomerated Bubbles, Gas Pocket, and Segregated Flow.

Since the ESP performance is closely linked to the flow pattern, it is crucial to identify the phase arrangement within the impeller. However, manually identifying these patterns for a large test matrix can be labor-intensive and necessitates heavy expertise. In this context, the utilization of artificial intelligence tools holds significant relevance for the analysis of these images. Several studies have been working on the development of neural networks to identify flow patterns. Dhillon and Verma (2019) presents that Convolutional Neural Networks (CNN) are mainly used for classification and image recognition, such as finding patterns that the human eye cannot process. Cerqueira *et al.* (2023) developed a CNN method to detected oil drops in two-phase oil–water dispersions within a centrifugal pump impeller. The author describes a specific architecture for a CNN, containing an input layer, responsible for receiving the captured images, multiple convolutional and pooling layers and an output layer.

The objective of this study is to experimentally investigate the impact of the number of stages on ESP performance operating with a gas-liquid mixture. To achieve this, an experimental apparatus was developed along with a prototype ESP. This setup enables visualization within the impeller and accurate measurement of the pump's performance parameters stage by stage.

The main contribution of this study is to conduct the comparison of ESP performance with varying numbers of stages and to establish a relationship between these measurements and the flow topology within the visualization impeller. The experimental methodology employed aims to isolate the effect of the stage number by ensuring consistent pressure conditions at the inlet of the visualization stage. As a result, flow pattern maps are presented as a function of operational conditions and stage numbers.

The experimental tests were conducted using a water-air mixture in four different stage configurations. The methodology employed both surging and mapping tests to obtain comprehensive data and insights into the performance of the ESP under different conditions.

2. EXPERIMENTAL FACILITY

Experiments were performed using the facility presented in Figure 1. The experimental apparatus is composed of water and compressed air circulation lines, separation tank, booster pump, temperature control system, measuring instruments, data acquisition system, in addition to an ESP centrifugal pump prototype.

In the experimental facility, a booster pump draws water from the separation tank; the liquid flows through the heat exchanger and the Coriolis meter and then reaches the suction of the pump prototype. At the same time, compressed air is injected into the liquid stream at the prototype's inlet. The gas-liquid mixture is then pumped to the separation tank, where the air is gravitationally separated, while the water returns to its line, in a closed loop. Both the booster pump and the pump prototype are driven by variable speed drives (VSD), which allows the shaft speed adjustment and, consequently, the flow control. Furthermore, control valves assist in regulating the line's pressure and the flow rates for each phases.

The pump prototype is based on a real ESP, model P23. To study the effects of the number of stages on the gas-liquid performance, the pump underwent modifications to enable visual access to the flow within the impeller and at pump intake; and measure the pressure stage-by-stage. Assembled in the vertical orientation, i.e, vertical upward flow, the pump prototype supports four different configurations with 1, 2, 3 or 4 stages. For simplicity, each configuration has been assigned a specific name: M1 for the setup with 1 stage, M2 for 2 stages and so forth. Figure 2 shows the setups M1 to M4.

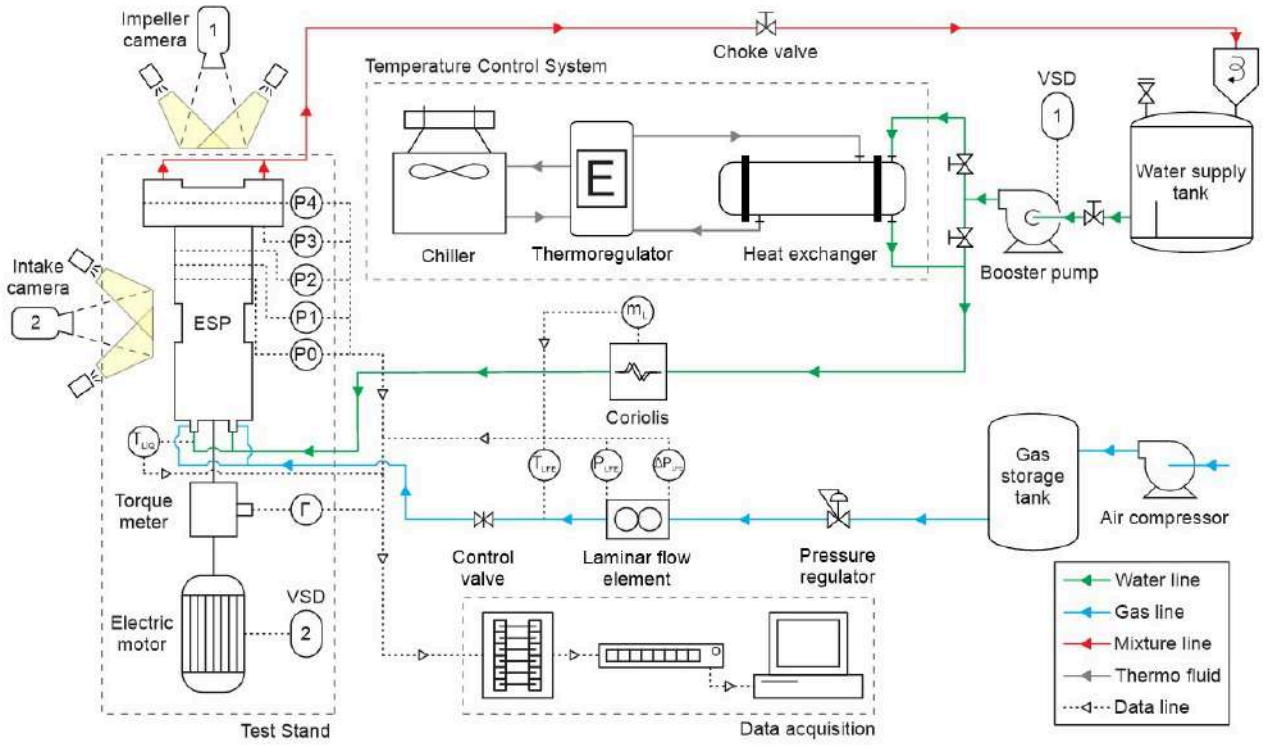

Figure 1: Schematic representation of the experimental apparatus.

To enable pressure measurements at each stage, five pressure taps were incorporated into the pump casing. These pressure taps communicate with the impellers eyes, through holes drilled in the diffusers. Since the outlet of one stage is the inlet for the downstream stage, this assembly allows the measurement of both inlet and outlet pressures for each individual stage.

Regardless of the configuration, the visualization stage is always the last stage of the assembly. For instance, in the M4 assembly with 4 stages, the visualization stage is the fourth stage. In the assembly with 3 stages, one standard stage is removed, and the visualization stage becomes the third stage. Therefore, the visualization stage always provides visual access to the impeller of the last stage. In this way, it is possible to visualize and measure the influence of the upstream stages on the visualization stage. In addition to the visualization stage, there is another viewing window placed at the inlet of the pump prototype, enabling the identification of the inlet flow pattern.

Two high-speed cameras were used simultaneously to visualize the pump intake and the visualization impeller. The

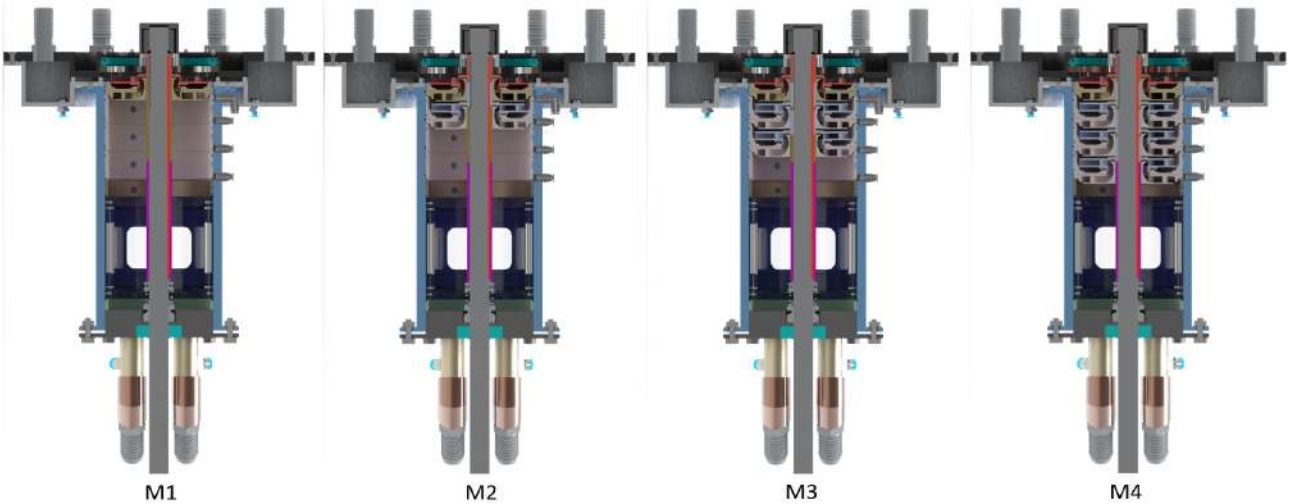

Figure 2: Pump prototype assemblies.

high-speed camera installed at the visualization impeller, a VEO 640S model, is capable of capturing up to 1400 frames per second at a resolution of 2560 pixels x 1600 pixels. Similarly, the camera installed at the pump intake, a VEO 340L model, is capable of capturing up to 800 frames per second at the same resolution. Both cameras are manufactured by Phantom®. Figure 3 shows the assembly of cameras for visualizing the impeller (1) and the pump intake (2).

Figure 3: High-speed cameras setup.

The experimental procedures used to study the pump's performance under gas-liquid flow include the surging and mapping tests. In the surging test, the liquid flow rate is held constant while the gas flow rate is increased. Consequently, the gas fraction increases along the performance curve. For the surging test three rotational speeds were used, 900, 1200 and 1500 rpm, and the water flow rates shown in Table 1. These liquid flow rates are related with the Best Efficiency Point (BEP) for each rotational speed, i. e., 0.6, 0.8, 1.0, 1.2 and 1.4 times the BEP.

Table 1: Surging test matrix

Rotational speed [rpm]	Liquid flow rate [m³/h]				
	0.6BEP	0.8BEP	BEP	1.2BEP	1.4BEP
900	2.33	3.10	3.88	4.66	5.43
1200	3.10	4.14	5.17	6.21	7.24
1500	3.88	5.17	6.47	7.76	9.05

In the mapping test, the gas flow rate is maintained constant while varying the liquid flow rate within an expected range, from the open-flow point (zero pressure gain) to the shutoff point (zero flow rate). Consequently, the gas fraction also increases with the reduction of the liquid flow. The mapping test used the same rotational speed of 900, 1200 and 1500 rpm, along with five different gas flow rates: 0.025, 0.050, 0.075, 0.100 and 0.125 kg/h.

This experimental matrix for surging and mapping tests is repeated for each pump assembly, i.e., M1, M2, M3 and M4. Therefore, the experimental for this two procedures and assemblies encompasses a total of 120 experimental curves.

For both experimental procedures and all assemblies, the pressure at the inlet of the visualization stage is maintained constant at 150 kPa (gauge). This approach is employed to isolate the effects of upstream pressure and number of stages on the visualization stage. By keeping the pressure at the inlet of the visualization stage constant, only the mixing effect caused by the upstream stages is considered in the flow.

This procedure differs from those described in the literature, where the overall performance of the pump with different numbers of stages is compared. As a result, it becomes challenging to differentiate between the mixing effects induced by the stages and the gas compression effect throughout the stages.

3. RESULTS

The results presented in this section refer to the performance of the visualization stage, i.e, with pressure increment defined as $P_4 - P_3$ (P4 and P3 being, respectively, the discharge and inlet pressure of the visualization stage, as seen in Fig.

1). Figure 4 shows a performance graphic of the visualization stage under water single-phase flow, different speeds and assemblies. This data provides a baseline for quantifying the performance degradation during gas-liquid flow. Analysis of single-phase testing is carried out based on the laws of similarity. The dimensionless head (ψ) and dimensionless flow rate (ϕ) are :

$$\psi = \frac{(P_4 - P_3)}{\rho\omega^2 D^2} \tag{1}$$

$$\phi = \frac{q}{\omega D^3} \tag{2}$$

where P is the pressure, ρ is the density, ω is the rotational speed, D is the impeller diameter, and q is the flow rate.

For negligible viscosity effects, the dimensionless head is a unique function of the dimensionless flow rate. Based on the obtained results, it is observed that the pump performance follows the same trend regardless of rotational speed and assembly. This indicates that the similarity laws hold true, and the influence of viscous effects is insignificant compared to the effects of the centrifugal field at different rotational speeds.

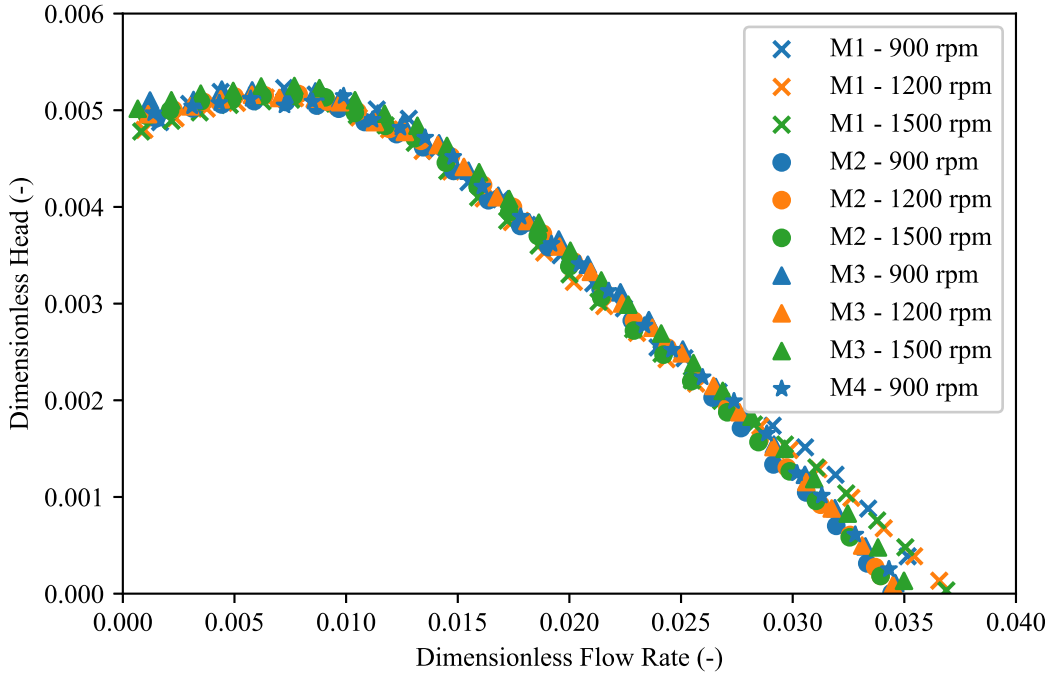

Figure 4: Single-phase flow experiments

Figure 5 presents the results of mapping tests for 900 rpm, assemblies M1, M2, M3 and M4, and five different gas flow rates. The different colors indicate the flow pattern classified with the aid of the mentioned CNN in the visualization impeller, i.e. blue is dispersed bubble, orange is gas pocket, and green is segregated flow pattern.

Figure 6 shows an example of each flow pattern identified within the visualization impeller.

Early on the performance curve, characterized by high liquid flow rates and low gas fractions, the Dispersed flow pattern is observed. In this flow pattern, the dispersed gas bubbles follow a path next to the liquid particles, without exhibiting any significant trend of accumulation. Additionally, there is no significant influence on pump energy transfer to the mixture and the performance is similar to each other regardless of gas flow rate. The degradation of pump performance begins near the transition from Dispersed to Gas Pocket flow pattern. Within this region, there is a greater population of bubbles, resulting in increased interaction between them. Initial indications of gas accumulation inside the impeller are observed due to stagnation of the bubbles and the forces balance, which tend towards equilibrium.

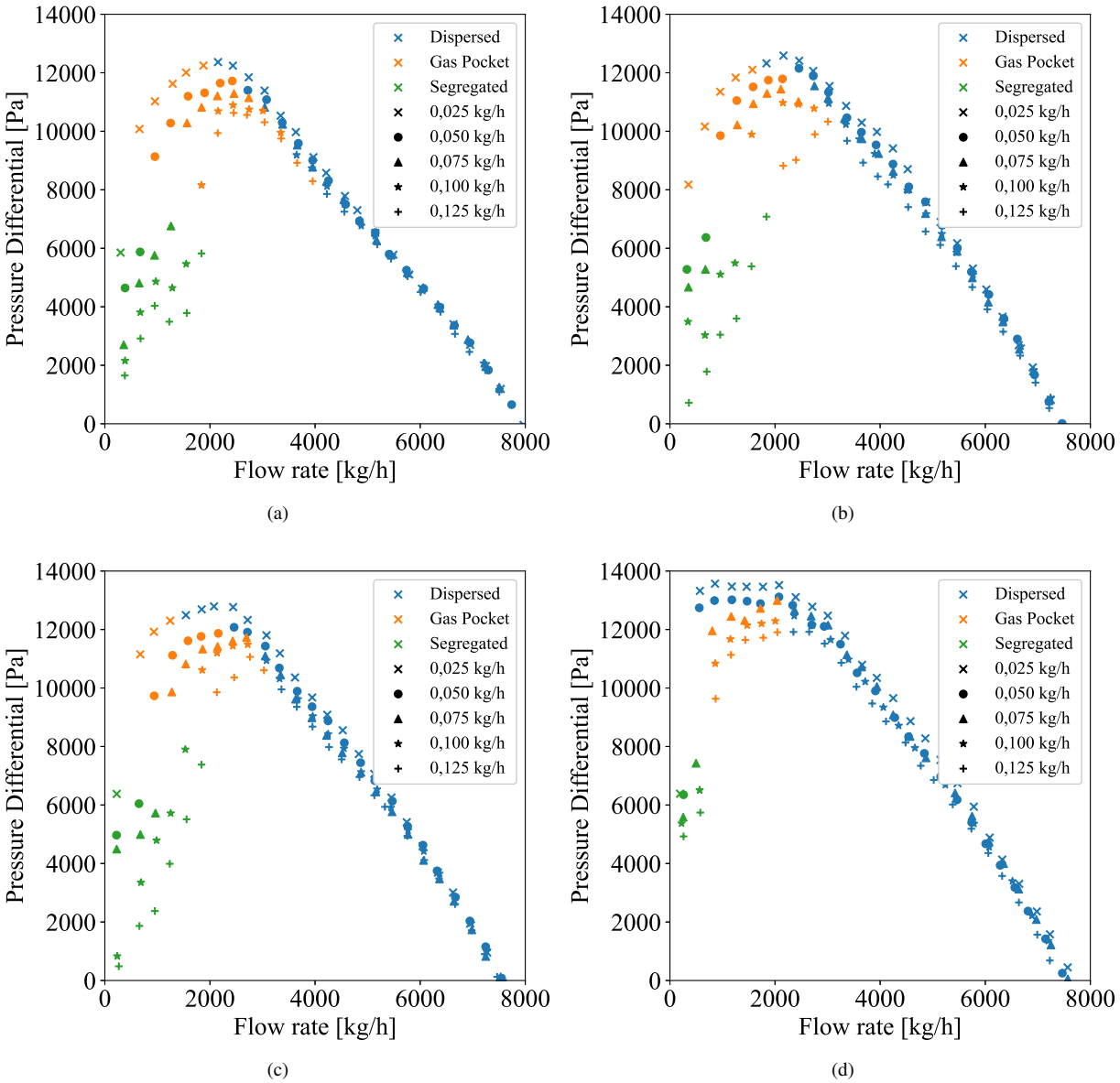

Figure 5: Mapping tests at rotational speed of 900 rpm, on setup: (a) M1, (b) M2, (c) M3 e (d) M4.

The performance curve reaches a maximum point and undergoes a change in trend. This maximum point introduces instability into the operation of the pumping system. The pressure curve required by the system can intercept the pump performance curve at more than one point, leading to instabilities. Operational instability is characterized by cyclic fluctuations in the measurement of performance parameters. This instability is commonly known as Surging. So, the flow pattern associated with the intensification of performance degradation and the Surging is the Gas Pocket flow pattern.

After reaching the maximum point on the performance curve, the pump's ability to generate head sharply decreases, leading to the occurrence of Segregated flow. Under this operational condition, the differential pressure across the pump becomes practically zero. This phenomenon is referred to as Gas Locking. However, despite the pressure differential being zero, there is still a non-zero liquid flow. This is attributed to the booster pump, which maintains a constant suction pressure for the main pump. The pressure differential created by the booster pump ensures the continuous flow of liquid. For this flow pattern the gas phase becomes continuous, resulting in flow segregation. A significant portion of the impeller channel is occupied by gas, and elongated gas bubbles tend to remain stationary within the impeller, occupying a considerable area of the transversal section of the channel.

Figure 7 shows the gas-liquid performance curve obtained from a mapping test conducted at 900 rpm, with gas flow rate of 0.125 kg/h. The results are shown for assemblies M1, M2, M3, and M4. The different colors also indicate the flow pattern observed in the visualization impeller.

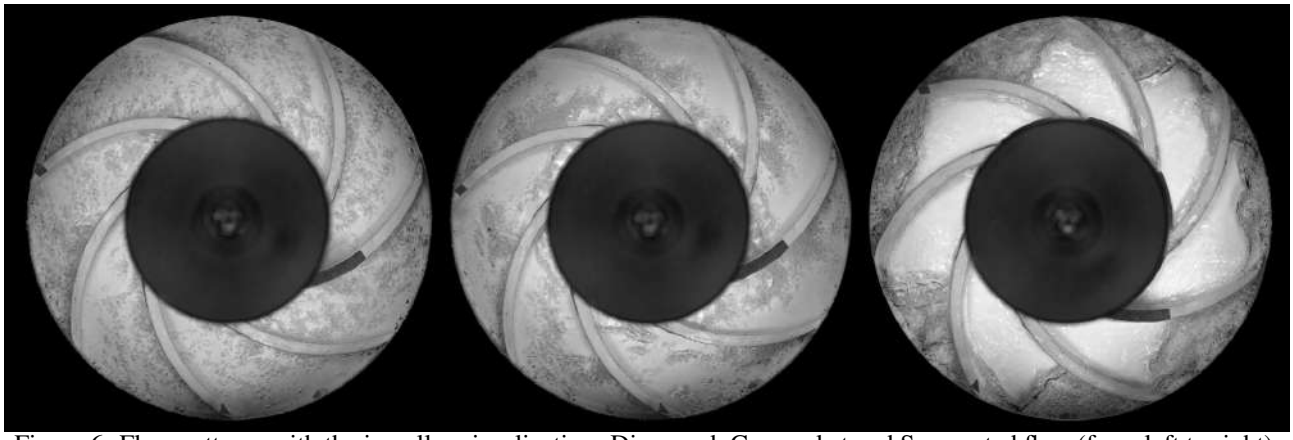

Figure 6: Flow patterns with the impeller visualization: Dispersed, Gas pocket and Segregated flow (from left to right).

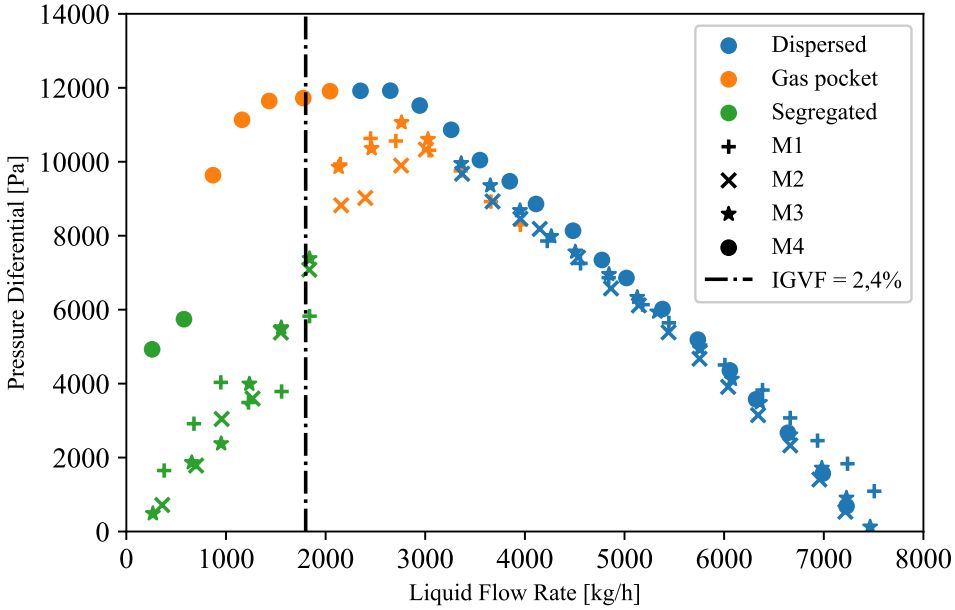

Figure 7: Mapping test curves at 900 rpm, 0,125 kg/h of gas flow rate and assemblies M1, M2, M3 and M4.

Under these experimental conditions, a direct correlation between the number of stages and the pump's performance is observed. It is evident that as the stage number increases, there is a noticeable improvement in the pump's performance. Furthermore, the number of stages also influences the operational condition where surging occurs. For example, the assembly with 4 stages (M4) can handle a higher gas fraction before reaching the surging point compared to M1.

The performance difference can be understood by observing the flow morphology within the visualization impeller. Figure 8 shows the images obtained with a high-speed camera at a homogeneous gas void fraction of 2.4% and a liquid flow rate of approximately 1800 kg/h. Two different flow patterns are observed: in M4, there is an early transition from dispersed to gas pocket flow, while assemblies M1, M2, and M3 show a segregated flow pattern.

The flow pattern observed in the images contributes to explaining the difference in pump performance. The gas pocket flow pattern is associated with the occurrence of the surging phenomenon and typically happens around the maximum point of the mapping curve. On the other hand, the segregated flow pattern severely impairs pump performance, significantly reducing the ESP's capacity to generate head.

Possibly, the greater capacity of the M4 assembly to handle gas occurs due to the mixing effect promoted by the upstream stages. Despite not contributing to an increase in pressure, these upstream stages are capable of generating sufficient turbulence levels, which effectively reduce the size of the gas bubbles at the entrance to the visualization stage.

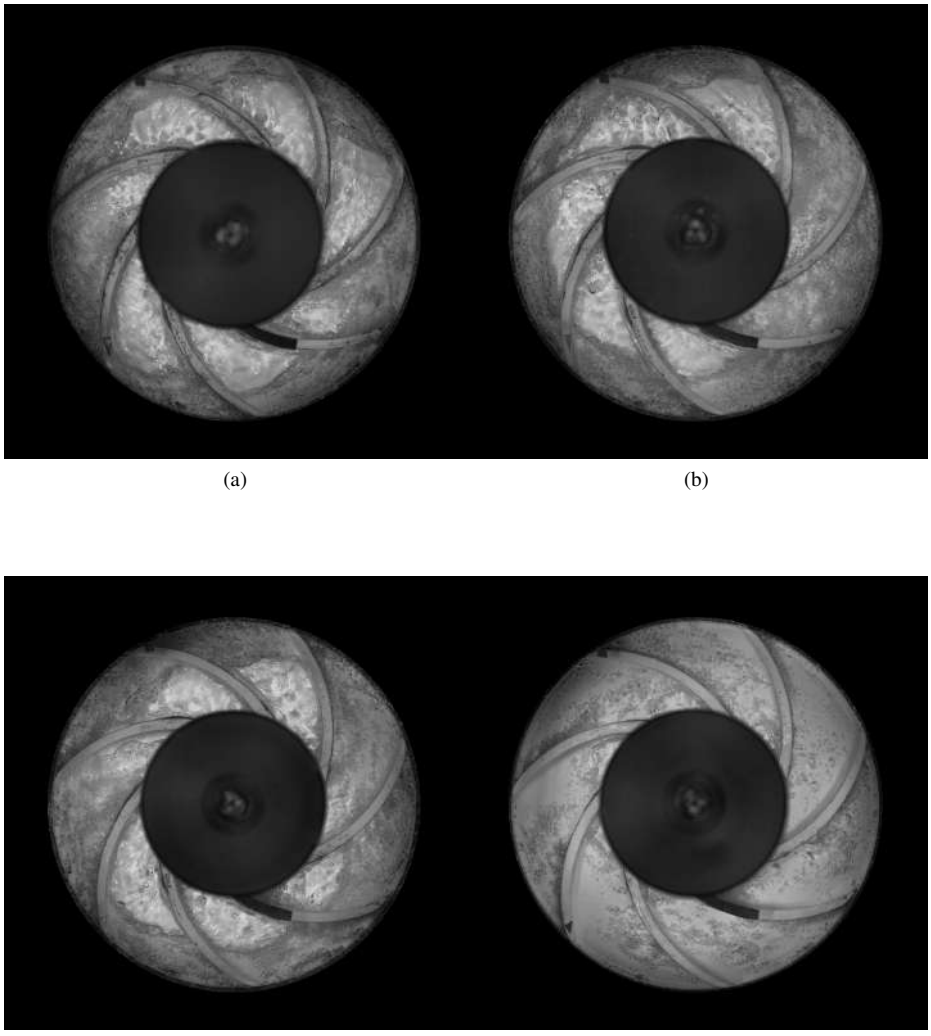

(a) (b)

(c) (d)

Figure 8: Flow visualization at 900 rpm, gas flow rate of 0,125 kg/h and IGVF = 2,4%, on setups: (a) M1, (b) M2, (c) M3 e (d) M4.

Figure 8 also reveals the difference between the flow pattern observed in M1 when compared with M2 and M3, in which larger gas bubbles are far more developed in the single-stage assembly. Providing the information that, despite displaying the same pattern, its characteristics are slightly different

Figure 9 shows the gas-liquid performance curve obtained from a mapping test at 1200 rpm, with a gas flow rate of 0.125 kg/h, and assemblies M1, M2, M3, and M4. The dashed-dotted line also represents a homogeneous gas void fraction of 2.4%. Under this operational condition, it is evident that the assembly has no significant impact on the pump performance and flow pattern within the visualization impeller. The performance curves and flow patterns show remarkable similarity across different assemblies.

In general, for the studied test matrix, the influence of the number of stages was only observed at a rotation speed of 900 rpm. However, for rotational speeds of 1200 and 1500 rpm, a notable impact of the assembly on the two-phase performance of the visualization stage was not observed.

This observation is supported by the results presented in Fig. 10 which includes all data points collected at 900 rpm for both mapping and surging tests. The circles represent the results obtained from the mapping tests, i.e, horizontal trends, where the gas flow rate is kept constant. On the other hand, the crosses indicate the results obtained from the surging tests, i. e. vertical trends, where the liquid flow rate is held constant. The colors also represent the flow patterns identified in the visualization impeller, similar to the previous results. These results can be interpreted as flow pattern maps for the pump impeller, facilitating the identification of transitions between different flow patterns.

Analyzing the results shown in Fig. 9, it is observed that, consistent with previous findings, configurations with more stages exhibit a reduced likelihood of performance degradation in the presence of free gas. This is evidenced by the flow pattern transitions shifting towards the left of the graph as the stage number increases. Another important result is that the mapping and surging tests behave, mostly, in a similar way, except for a few separate occasions.

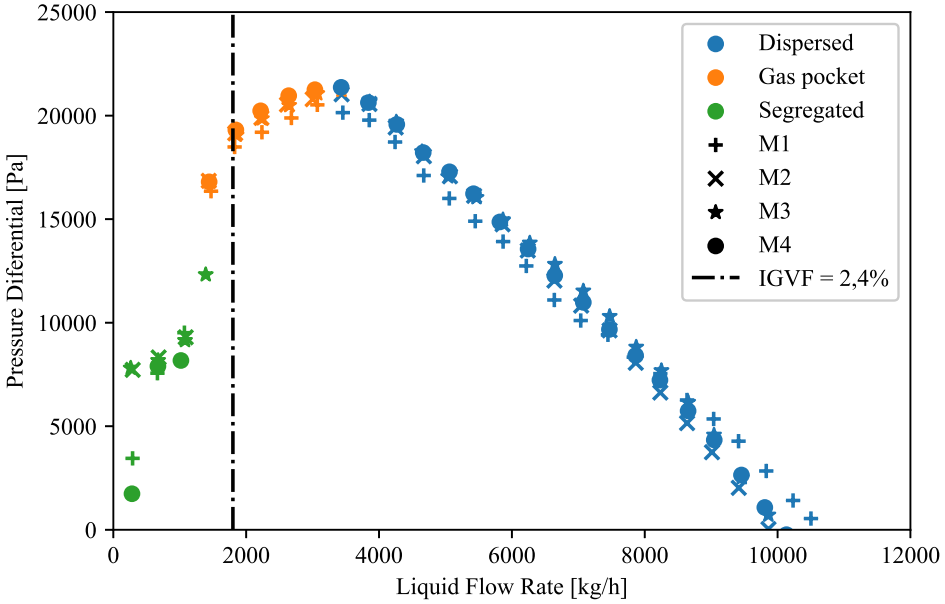

Figure 9: Mapping test curves at 1200 rpm, 0,125 kg/h of gas flow rate and assemblies M1, M2, M3 and M4.

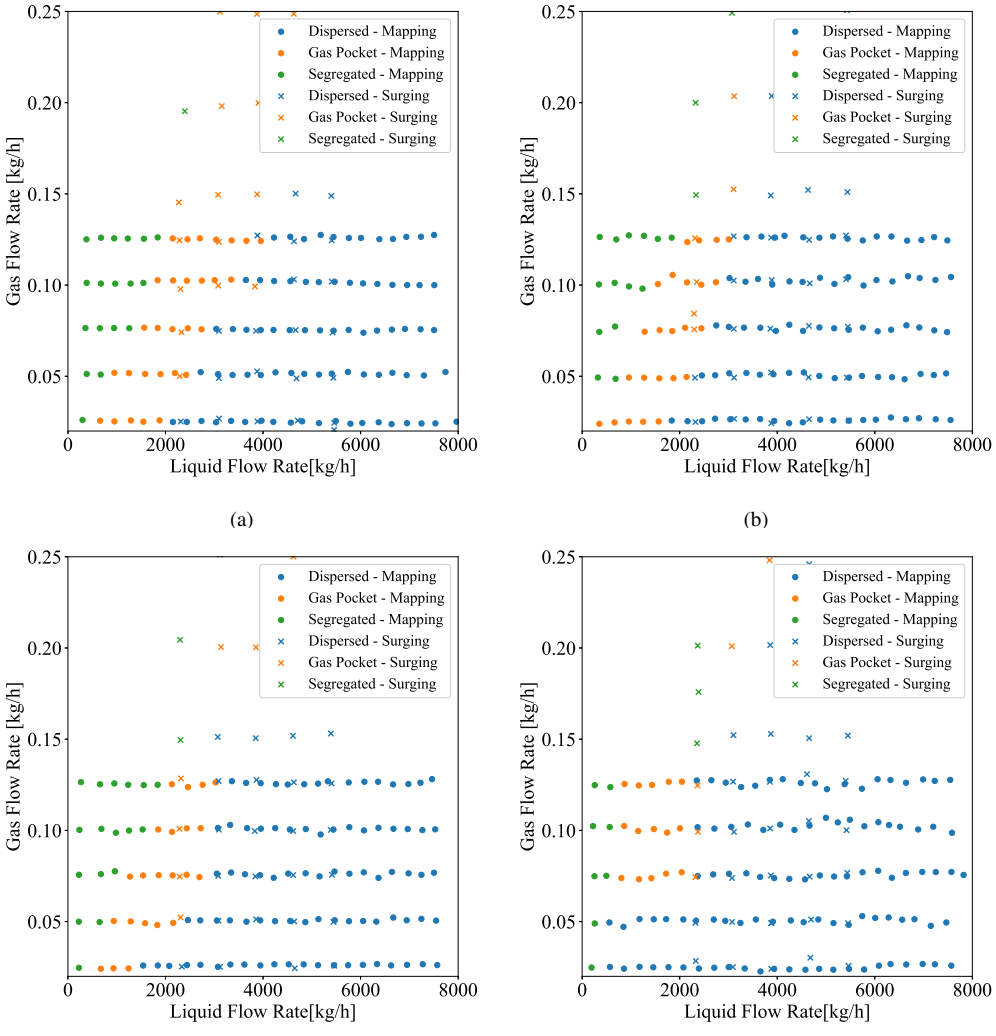

Figure 10: Surging and Mapping tests at 900 rpm, gas flow rate on the y axis and liquid flow rate in x, setups: (a) M1, (b) M2, (c) M3 e (d) M4.

4. CONCLUSION

A series of experimental tests were conducted in order to investigate performance characteristics of an Electric Submersible Pump under various conditions, mainly in order to understand the effects of different stage number. The test matrix encompassed multiple different parameters such as pump rotational speeds, gas and liquid flow rates.

The findings present in this work revealed that the number of stages in the pump directly impacts its performance at low rotational speeds. The flow visualization study provided evidence that the presence of segregated flow patterns has a significant impact on the pressure differential of the pump. Moreover, it was observed that the occurrence of gas pocket flows serves as an indicator of surging, which is the point at which the pump begins to lose its capacity to generate pressure. This underscores the critical role played by the flow pattern in determining the optimal flow rates for a better performance. Another important observation possible through the visualization section is that there are significant differences in the flow patterns, despite being characterized as the same.

Furthermore, the analysis demonstrated that configurations with more stages exhibited greater resistance to performance degradation in the presence of gases at 900rpm. The transition from dispersed bubbles to gas pockets was highly dependant on the liquid flow rate, with higher stage count configurations requiring a higher intake gas void fraction for this transition to occur. Notably, at the 4 stage ESP configuration (M4) the gas pocket flow pattern did not occur for two different gas flow rates, 0.025 and 0.050 kg/h. This highlights how a higher number of stages can effectively minimize degradation by acting as a gas handler. By incorporating the gas into the liquid, a mixture with smaller bubbles is produced, thereby enhancing the pump's capacity to generate head pressure, particularly under gassy conditions.

When comparing mapping and surging tests, it was evident that similar patterns emerged, highlighting the significance of comprehending and managing flow patterns within the pump's impellers. Despite the presence of comparable flow patterns at the intake, different performance outcomes were observed. This emphasizes the necessity for a deeper understanding of two-phase gas liquid flows within Electric Submersible Pumps.

Overall valuable insights were gained from this study into the performance of ESP with different configurations related to the number of stages. Further research and analysis is needed to expand upon these findings, specially for higher gas flow rates in mapping tests and a wider experimental matrix, with different fluids. The knowledge obtained from this study can further expand upon designing ESPs.

5. REFERENCES

Cerqueira, R.F., Perissinotto, R.M., Monte Verde, W., Biazussi, J.L., de Castro, M.S. and Bannwart, A.C., 2023. "Development and assessment of a particle tracking velocimetry (PTV) measurement technique for the experimental investigation of oil drops behaviour in dispersed oil–water two-phase flow within a centrifugal pump impeller". *International Journal of Multiphase Flow*, Vol. 159, p. 104302.

Cirilo, R., 1998. *Air-water Flow Through Electric Submersible Pumps*. Artificial Lift Projects research report. University of Tulsa. URL `https://books.google.com.br/books?id=EPcROAAACAAJ`.

Dhillon, A. and Verma, G., 2019. "Convolutional neural network: a review of models, methodologies and applications to object detection". *Progress in Artificial Intelligence*, Vol. 9. doi:10.1007/s13748-019-00203-0.

Gamboa, J., 2009. *Prediction of the transition in two-phase performance of an electrical submersible pump*. Ph.D. thesis, University of Tulsa.

Gamboa, J. and Prado, M., 2011. "Review of electrical-submersible-pump surging correlation and models". *SPE Production & Operations - SPE PROD OPER*, Vol. 26, pp. 314–324. doi:10.2118/140937-PA.

Monte Verde, W., 2016. *Modelagem do Desempenho de Bombas de BCS operando com Misturas gás-óleo viscoso*. Ph.D. thesis, Tese (Doutorado) , Universidade Estadual de Campinas, Campinas.

Zapata, L.C., 2003. *Rotational speed effects on ESP two-phase performance*. Ph.D. thesis, University of Tulsa.

Zhu, J., Zhu, H., Cao, G., Zhang, J., Peng, J., Banjar, H. and Zhang, H.Q., 2019. "A new mechanistic model to predict boosting pressure of electrical submersible pumps esps under high-viscosity fluid flow with validations by experimental data". *SPE Gulf Coast Section Electric Submersible Pumps Symposium*. doi:10.2118/194384-MS. URL `https://doi.org/10.2118/194384-MS`.

6. RESPONSIBILITY NOTICE

The authors are solely responsible for the printed material included in this paper.

7. ACKNOWLEDGEMENT

The authors of this work would like to acknowledge Petrobras and ANP (grant number: 2017/00763-5) for financial support.